Received: 13 December 2021 | Revised: 23 January 2022 | Accepted: 24 February 2022

DOI: 10.1002/jcc.26834

RESEARCH ARTICLE

Journal of COMPUTATIONAL CHEMISTRY WILEY

# A real space picture of the role of steric effects in $S_N2$ reactions

Miguel Gallegos | Aurora Costales | Ángel Martín Pendás

Department of Analytical and Physical Chemistry, University of Oviedo, Oviedo, Spain

**Correspondence**
Ángel Martín Pendás, Department of Analytical and Physical Chemistry,University of Oviedo, E-33006, Oviedo, Spain.
Email: ampendas@uniovi.es

**Funding information**
Ministerio de Ciencia e Innovación, Grant/Award Numbers: FPU19/02903, PGC2018-095953-B-I00

## Abstract

Within substitution reactions, the Bimolecular Nucleophilic Substitution ($S_N2$) reaction mechanism is one of the most frequently found and studied ones. Among other factors, the easiness of the $S_N2$ pathway is classically considered to be determined by steric hindrance. However, the diffuse nature of the latter inevitably darkens these and other arguments holding the pillars of chemical intuition. In this work, we employ the steric energy ($E_{ST}$) descriptor, formulated within the Interacting Quantum Atoms approach, to offer insights regarding this problem. The steric demands of the substrate, nucleophile and leaving group were studied using the gas-phase $S_N2$ reaction with different organic skeletons ($CH_3$—, $CH_3CH_2$—, $(CH_3)_2CH$—, $(CH_3)_3C$—, $(CH_3)_3CCH_2$—) and halogens (F, Cl, and Br) as test-bed systems. Our results show that, according to $E_{ST}$, the SH experienced along these simple reactions fits, in the general case, the trends predicted by a meticulous and rigorous application of chemical intuition. However, steric clash alone should not be considered as the only argument used to explain the easiness of the $S_N2$ reaction over different electrophiles.

**KEYWORDS**
bimolecular nucleophilic substitution, chemical reactivity, interacting quantum atoms, quantum theory of atoms in molecules, steric repulsion

## 1 | INTRODUCTION

Substitution reactions, involving the exchange of two functional groups within a given chemical skeleton or substrate, are fundamental chemical processes with huge implications in chemical reactivity and synthetic strategies.[1–4] One of the apparently simplest, and yet fundamental, plausible mechanism for these chemical transformations is the so-called bimolecular nucleophilic substitution ($S_N2$), represented in Figure 1. This mechanistic proposal, as stressed by Ingold and coworkers,[5] involves the attack of a nucleophile (Nu) to an electrophilic center (E), usually a C atom exhibiting a strongly polarized bond as a result of the electronegativity difference with the neighboring atoms, that induced the formation of a new C—Nu bond with the concomitant extrusion of a chemical moiety, referred to as the leaving group (L), and hence the bond breaking of the original C—L bond. Under common circumstances, the $S_N2$ mechanism is considered to take place through the backside attack of the electrophile, leading to a characteristic Walden inversion of the substrate, though alternative proposals, such as the frontside $S_N2$ reaction or other more recently proposed mechanisms, such as the double inversion, have also been formulated.[6,7] Additionally, several side reactions are known[6,8,9] to compete with the substitution process, including elimination or even rearrangements transformations.

Due to its moderate size, simplicity and relevance, this and other similar reactions have been widely employed as model systems to unravel the nature of chemical bonding and reactivity.[10–12] The

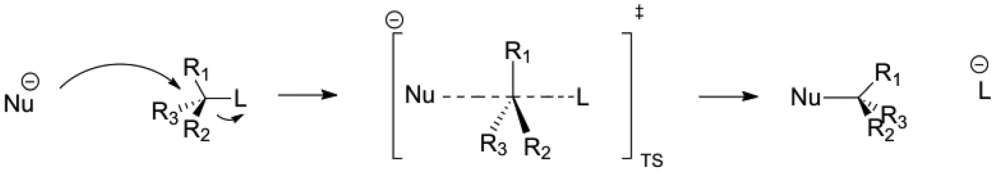


**FIGURE 1** Schematic representation of the general $S_N2$ reaction mechanism

archetypal example involves a substitution reaction of halogen-like groups taking place over a carbon based electrophile,[6] though substitution reactions of electrophiles of different chemical nature have also been explored.[13–16] Indeed, the $S_N2$ reaction constitutes one of the basic kernels of classical organic chemistry and it has been widely studied both computationally[17–34] and experimentally.[9,35–38] It is generally believed[4] that the feasibility of the bimolecular substitution reactions is determined by a combination of multiple factors, including the nature of the nucleophile and leaving groups, the skeleton of the electrophile and the solvent. Unfortunately, the actual role of some of these effects remains still unclear and under debate. For instance, the steric hindrance (SH) built upon the formation of the penta-coordinated transition state was originally considered to be one of the dominant driving forces leading to the observed reaction barrier. However, this explanation has been seriously questioned in recent years by some authors, including Fernández and co-workers[39] who pointed out the weakening of the stabilizing orbitalic interactions as the main origin of the observed reaction barrier, though such an approach has also been criticized.[40] Furthermore, steric terms have also been classically considered,[4,41] under the eyes of chemical intuition, as the main impediment preventing the bimolecular nucleophilic substitution over crowded electrophiles from taking place. For instance, as the electrophilic center gets increasingly crowded, so does, generally, the reaction barrier associated to this concerted process, something used to explain the lower tendency of secondary and tertiary substituted carbons to undergo $S_N2$ like transformations. Such a trend has been classically attributed to the *steric shielding* induced by bulky substituents in the electrophilic center, difficulting the backside attack of the nucleophile and favoring a stepwise mechanism, usually referred to as a $S_N1$ reaction,[5] in which the C—L bond is broken leading to the formation of a quasi-stable planar carbocation intermediate species.

Whether or not steric congestion is actually behind these and similar processes is still under debate, but its relevance in chemistry is beyond question. Unfortunately and despite its fundamental role in classical chemical models, SH is, along with other chemical terms, one of the so-called *chemical unicorns*,[42] concepts that lack from a direct observable and a rigorous definition but which are apparently well consolidated in the chemist's minds. The loose definition and vague nature of these terms has motivated the scientific community to unravel its true nature, if any. Indeed, a wide variety of computational tools and models have been employed in recent years to elucidate the origin of SH.[43–47] Following this trend, and drawing on the previous work developed by Popelier and co-workers,[43] we have recently shown[12] that a real space descriptor of steric effects, the so-called steric energy $E_{ST}$, can be easily obtained with the aid of the IQA energy partitioning scheme.[48] Such a descriptor is obtained by freeing the deformation energy ($E_{def}$) of an atom or fragment from its charge transfer component ($E_{CT}$). It is worth mentioning that our approach prevents any of the well described[49] indefinitions and inconsistencies attributed to the usage of fictitious intermediate and references states, required by other analysis techniques, leading moreover to an orbital invariant picture.

Considering the success of real space techniques in the analysis of some simple substitution reactions,[11,12] in this work we try to shine light on the actual role that SH plays in the latter, studying in detail the effect of the steric demands of the nucleophile, electrophile and leaving groups. Furthermore, in the latter case, special attention is paid to the distinctive effect of the geminal and vicinal groups belonging to the substrate. For such a purpose, a collection of halogen exchange reactions was studied in the gas phase with different nucleophile and leaving groups (F, Cl, and Br) and substrates ($CH_3$—, $CH_3CH_2$—, $(CH_3)_2CH$—, $(CH_3)_3C$—, and $(CH_3)_3CCH_2$). It is worth mentioning that though substitution reactions are usually carried out in solution and the effect of the solvent in its dynamics is beyond question,[4,50,51] solvent effects will not be addressed in this work. Modeling the reaction in the vacuum comes as a reasonable approximation in order to study exclusively the effects of SH. Moreover, and although solvent effects have been claimed to modify substantially SH throughout the reaction,[21,52] it has also been stressed that geometries are only modified to a minor extent[52] and thus our model systems should yield chemically representative and meaningful results. The work is organized as follows: first a brief overview of the concept of steric energies, $E_{ST}$, within the context of the IQA partitioning scheme is presented. Then the SH and steric effects attributed to the substrate, nucleophile and leaving group along the studied gas-phase transformations are discussed. The final section gathers the conclusions drawn from this work.

## 2 | THE STERIC ENERGY ($E_{ST}$) DESCRIPTOR OF SH

The diffuse origin and nature of SH has crystallized in the development of a wide variety of tools and models for the measurement of steric congestion. Indeed, many different formalisms have been used for the previous purpose, including Symmetry Adapted Perturbation Theory (SAPT),[53] the Natural Bond Orbital (NBO) method[54] and energetic partitioning schemes, such as the Energy Decomposition Analysis (EDA)[55] and the IQA[48] approaches, to name just a few. It is precisely within the latter approach, where the steric energy, $E_{ST}$, descriptor was derived.[12] The IQA approach is a real-space based technique, formulated within the Quantum Theory of Atoms in

Molecules (QTAIM) theory,[56] which decomposes the total energy of any chemical system as a sum of one- and two-body energy terms, named self and interaction energies, respectively, as:

$$E = \sum_A E^A_{self} + \frac{1}{2}\sum_{A,B\neq A} E^{AB}_{int}. \quad (1)$$

Moreover, the two contributions appearing in the previous expression can be further partitioned in physically sound terms whose discussion is out of the scope of this work. Since the self or net energy of an atom or fragment is inherent to such an entity, it is generally expected to be only slightly modified by a perturbation of its environment. Thus, the evolution of the self-energy upon the interaction between two chemical moieties is more adequately measured with respect to a suitable reference, resulting in the so-called deformation energies, $E^A_{def}$,:

$$E^A_{def} = E^A_{self} - E^A_{ref}, \quad (2)$$

where $E^A_{ref}$ is the self-energy of the QTAIM region A in its reference state, as for instance the isolated moiety in the vacuum. Under common scenarios, deformation energies exhibit a positive and exponentially increasing trend with the confinement or compression of a system, something which has led some authors[43] to conclude that such an energy term is actually able to measure steric congestion. Unfortunately, the strong dependence of the net or self-energy of an atom with a change in its electron count, makes the previous approach not general, something which is clearly evidenced, for instance, in the inability of $E_{def}$ to represent the SH of H atoms. Thus, a more suitable descriptor of steric congestion can be derived by removing the charge transfer contribution, $E_{CT}$, from the total deformation energy, as:

$$E^A_{ST} = E^A_{def} - E^A_{CT}. \quad (3)$$

Furthermore, the charge-transfer term can be rigorously computed within the Grand-Canonical DFT formalism[57] from the successive ionization potentials of the species under consideration (see Table S11 for further details). Altogether, this geometrical deformation, or simply steric energy, has been proven[12] to provide a more faithful and general picture of the steric congestion than plain deformation energies, even in the peculiar case of highly charged H atoms.

## 3 | COMPUTATIONAL DETAILS

All calculations were performed in the gas phase, without relativistic corrections, at different levels of theory, including HF and DFT in combination with the aug-cc-pVDZ basis set. Geometry optimizations, frequency calculations, single point calculations and intrinsic reaction coordinate (IRC) paths were computed using the Gaussian09 quantum chemistry package.[58] Similarly, the wavefunctions corresponding to each point along the computed reaction path were generated with the aid of Gaussian09.[58] On the other hand, IQA calculations were performed using the in-house made PROMOLDEN code.[59] Further details about the energetic partitioning calculations can be found in the Supporting Information (SI). As far as DFT is regarded, the Minnesota functional M06-2X[60] was employed as implemented in Gaussian09.[58] Since the steric energy is known to be barely dependent on the methodology,[12] at least at a qualitative level, the levels of theory employed throughout this work were chosen on the basis of experimental data reproducibility. Indeed, the selection of the combination of such a functional and basis set was achieved after a small benchmarking study performed in one of our previous works,[12] which showed that such a level of theory is capable of accurately reproducing experimental reaction barriers of common halogen substitution reactions. Although it is clear that geometries are important when dealing with steric congestion, given that our SH descriptor is energetic we have preferred energy over geometric performance on choosing the functional/basis set combination. For the sake of convenience and clarity, IRCs and similar calculations are many times reported as relative ratios or percentages of the reaction coordinate value ($\chi$), where $-1$ and 0 correspond to the starting reactive complex and the transition state structure, respectively. All the energies and charges presented in this work are reported as relative values using the suitable reactive complex as reference frame. Since the model reactions employed to study the effect of the substrate are thermoneutral, only one of the counterparts of the full IRC profile, from the reactants to the TS, was analyzed. It should be mentioned that in the particular case of the neopentyl substrate, the first three points along the IRC profile were discarded as a result of some numerical instabilities. Similarly, the last point in the reaction with the $(CH_3)_3C$ substrate was removed.

## 4 | RESULTS

### 4.1 | Effect of the substrate

In order to explore the previously mentioned steric shielding induced by the groups borne by the electrophilic center, the halogen self-exchange reaction was analyzed for a series of progressively bulkier substrates. For the sake of convenience and simplicity, all reactions were studied using F as both leaving group and nucleophile. As shown in Figure 2, and in agreement with already reported data,[24,61–63] the starting reactive species corresponds to an ion-molecular complex, leading to the double-well potential energy surface characteristic of gas phase nucleophilic substitutions over carbon based substrates. This behavior is, however, greatly diminished in polar solvents.[63]

Generally speaking, as the electrophilic center gets increasingly crowded, the reaction becomes less favorable, as reflected in Figure 3, that shows the evolution of the total electronic energy during the reaction for different substrates. Such a trend, corresponding to activation Gibbs Free Energies, $\Delta G^{\ddagger}$, of 14.5, 19.0, 23.8, 28.8, and 19.6 kcal/mol, respectively (see SI Section 2, Table S1 and Figures S1–S2) is in good agreement with chemical intuition.[4,5] The

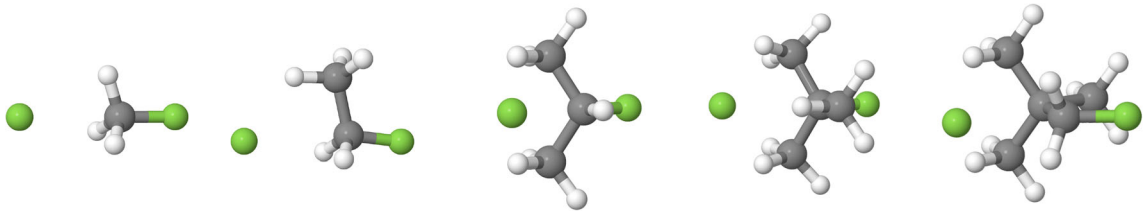

**FIGURE 2** Energetically minimized geometries, at the M06-2X/aug-cc-pVDZ level of theory in the gas phase, of the reactive complex involved in the self substitution reactions (Nu = L = F) for different substrates: $CH_3$—, $CH_3CH_2$—, $(CH_3)_2CH$—, $(CH_3)_3C$—, and $(CH_3)_3CCH_2$—

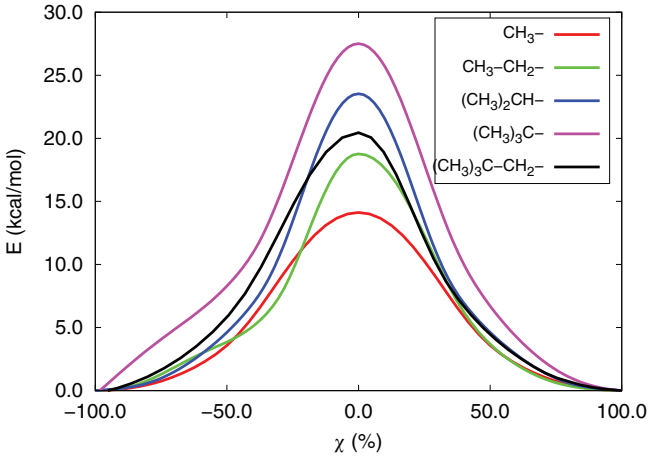


**FIGURE 3** Reaction energy profile of the self substitution reactions (Nu = L = F) with different substrates. The reported energies correspond to electronic energies computed at the M06-2X/aug-cc-pVDZ level of theory in the gas phase

nature of these observed trends has resulted in several debates in the literature. Although it was originally assumed to be a result of the increasing steric repulsion faced by the nucleophile, and this has been widely supported in the literature,[4,9,21,61–65] it has been recently claimed that the depletion of favorable stabilizing interactions may also play a critical role.[39,66–68] Furthermore, it is particularly interesting to analyze the case of the neopentyl fluoride ($(CH_3)_3CCH_2F$) which, despite being a primary substituted electrophile, behaves similarly to a secondary substituted species, something which could be rationalized, at first sight, attending to the steric effects at the vicinal, and not geminal, position in well agreement with already reported results.[8,41,69]

It is worth mentioning that, despite being thermoneutral, the reaction profiles are not always perfectly symmetric with respect to the transition state. Such a slight asymmetry arises from secondary geometrical processes such as structural reorganization phenomena of the vicinal groups and it is hence more evident in electrophilic scaffolds bearing easily rotatable groups, such as methyl moieties. Additionally, the differences between both counterparts of the reaction profiles become even more prominent through the analysis of the reaction force experienced along the chemical transformation (see SI Section 7, Figure S27).

Figure 4 collects the evolution of the steric energy ($E_{ST}$) experienced by the different chemical fragments involved in the reactions under study. As far as the leaving group is regarded, there is a very clear and common behavior to all the substrates. Initially, the SH of the leaving group is barely modified, corresponding to a perturbative-like regime in which the C-L distance is almost unaltered (see SI Section 3.1) and in which a very subtle electron enrichment takes place (see SI Section 4.1). From this point on, the $E^{L}_{ST}$ decays quite rapidly, leading to a release of the steric congestion of about 40 kcal/mol that is accompanied by a significant electron enrichment (∼0.10 electrons, see SI Section 4, Table S2 and Figures S13–S15 for more details) on L, which can be rationalized attending to the C—L bond breaking process and the subsequent decompression of the leaving group. It is interesting to notice, however, that the overall steric release experienced by L is similar for any of the studied substrates, suggesting that it is nearly unaffected by the chemical environment of the electrophile. Such a result could be attributed to the small size and compactness of the fluoride anion ($F^-$), indicating that the SH experienced by this atom would mainly arise from the direct compression against the electrophilic center (C atom) while not being affected up to a significant extent by the remaining chemical scaffolds, which are moreover oriented towards the opposite face of the electrophile. Additionally, the evolution in the C—L bond distance varies very slightly with the nature of the substrate, exhibiting an increase of ∼0.10 Å throughout the series (see SI Section 3, Figures S3–S12).

On the other hand, the evolution of the SH experienced by the nucleophile exhibits a slightly more complex behavior, following a similar trend to that observed for the total deformation energy (see SI Section 5, Figures S16–S24). First of all, the $E^{Nu}_{ST}$ increases along the nucleophilic attack as a result of the nucleophile to electrophile compression but it does not follow, however, a uniform and steady increase rate. Whereas non-, primary- and secondary- substituted centers lead to maximum steric penalties of roughly 12.0 kcal/mol, the tert-butyl skeleton yields a considerably reduced $E^{Nu}_{ST}$. This result is in partial disagreement with chemical intuition,[4,5] according to which the nucleophile would be expected to face larger steric penalties with increasingly substituted electrophilic centers. Although counter-intuitive at first glance, such a finding can be perfectly rationalized after a meticulous inspection of the two main factors contributing to the total clashing of the nucleophile:

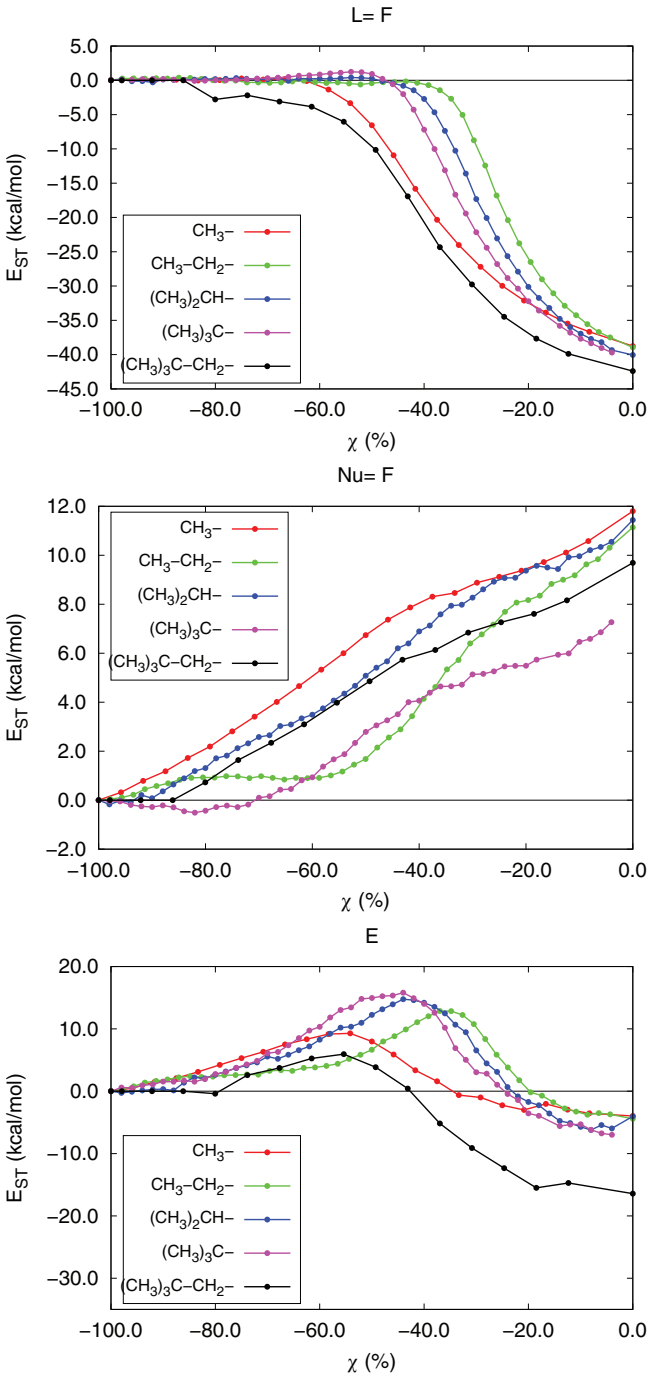


**FIGURE 4** Evolution of the steric energy $E_{ST}$ of the leaving group (top), nucleophile (center) and electrophile (bottom) for different substrates along the self substitution reactions (Nu = L = F). Calculations performed at the M06-2X/aug-cc-pVDZ level of theory in the gas phase

- Compression against the central C atom: a monotonically increasing term (*f*(d[C—Nu])) in the transition from reactants to the TS.
- Compression against the spectator (S) groups, geminal (G), or vicinal (V): a complex, and not easily predictable, contribution arising from the Nu—G or Nu—V clashing (see Figures S25–S26 for further details).

It is evident that whereas the first contribution can be equivalently compared for different skeletons, the same does not hold for the latter, owing to the different nature of the studied spectator groups. Accepting the classical chemical narrative[1] and accounting for the larger decrease in the C—Nu and C—S distances (0.9 and 0.4 Å) and bulkiness of the $(CH_3)_3C$- skeleton when compared to its $CH_3$ analog (undergoing bond shortenings of 0.7 and 0.3 Å, respectively), the aforementioned compression would be expected to be larger for the former. However, the $E_{def}$ and $E_{ST}$ energies are known[43] to exhibit, and specially under mild clashing scenarios, an exponentially decaying behavior with the distance. Within this regard, a direct comparison of the starting C—Nu and C—S distances reveals that the nucleophile in the starting reactive complex, taken as reference, is in much closer proximity (showing $\Delta d$ of about 0.3 and 0.4 Å, respectively) for the reaction with the $CH_3$ electrophile. Thus, and against our intuition, the further proximity of the Nu to the electrophile in the reaction with $CH_3F$ is likely to yield larger relative steric penalties for the former when compared to the bulkiest substrate.

Moreover, and unlike in the previous case, the C—Nu distance decreases quite uniformly along the reaction (see SI section 3), exhibiting an increase in the C—Nu bond shortening of about 0.30 Å through the explored substrate series. In order to understand these trends it is crucial to account for all the different, yet coupled, processes taking place and contributing to the congestion of the nucleophile. Initially, along the perturbative-like regime, the Nu approaches the electrophile in a linear fashion way and hence the compression against the central core of the substrate is the main factor contributing to its steric congestion. However, once the perturbative regime is abandoned (at around $\chi = [-0.6, -0.4]$) a strong geometrical deformation of the electrophilic center takes place, ultimately leading to a planar or quasi-planar disposition of the substrate central atom at the transition state, as shown in Figure 5. Such a geometrical distortion, involving the relative displacement of the chemical moieties directly attached to the central carbon atom towards the frontside face of the electrophile, results in a subtle reduction of the local compression experimented by the nucleophile. The previous fact explains why, once the perturbative regime is overcome, the rate of increase of the $E_{ST}^{Nu}$ along the reaction coordinate decreases slightly. However, a somewhat anomalous behavior is found for the methyl substituted ($CH_3$—$CH_2$—) substrate as shown in green in Figure 4, which exhibits a plateau in the evolution of $E_{ST}^{Nu}$, something that is also observed in a much minor extent in the reaction with the tertiary substituted C atom. In order to understand this discrepancy, a closer look to the evolution of the secondary geometrical distortions undergone by this system must be taken. Indeed, the distance of the nucleophile to the closest geminal atom shows two distinctive plateaus (see SI section 3), something which is moreover coupled to an internal rotation of the methyl group, that goes from a quasi-eclipsed to a staggered local disposition with respect to the nucleophile. These observations suggest that the carbon to nucleophile compression is partially counteracted by the reduction in the relative bulkiness of the geminal groups together with the partial planarization of the electrophile. It is precisely the interplay between these two opposite phenomena that

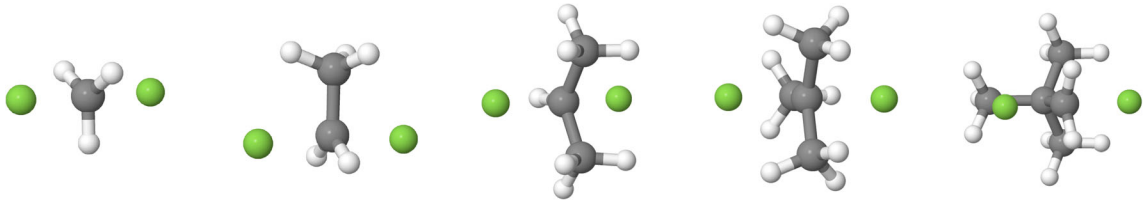

**FIGURE 5** Energetically optimized geometries, at the M06-2X/aug-cc-pVDZ level of theory in the gas phase, of the transition state involved in the self substitution reaction with different substrates: $CH_3$—, $CH_3CH_2$—, $(CH_3)_2CH$—, $(CH_3)_3C$—, and $(CH_3)_3CCH_2$—. Further details can be found in SI (Tables S3–S10)

explains the observed behavior. On the other hand, in the particular case of the $(CH_3)_3CF$ skeleton, the plateau found in the evolution of $E_{ST}^{Nu}$, appearing in the very infant reaction stages, is very likely to arise from the almost negligible exponential increase of $E_{ST}$ exhibited at this initial perturbative scenario. Something which is even more dramatic given the large nucleophile to electrophile distance found in the starting reactive complex for this system. Altogether, these findings are able to perfectly explain the somewhat intriguing trends found for the methyl and tert-butyl substituted skeletons.

It should be noticed that, unlike in the previous case, where the local environment of the electrophile was suggested to have a negligible effect in the steric decongestion experienced by the leaving group, the $E_{ST}^{Nu}$ seems to be affected significantly by it. Such a different behavior can be rationalized considering that the nucleophile approaches the electrophile through its backside and hence the former is in a much closer proximity to the different moieties directly bonded to the carbon atom. Additionally, the C—X distance in the activated complex species, with values of 1.82, 1.84, 1.88, 1.93, and 1.84 Å along the series, is nearly unaffected by the substrate, showing a very reduced bond elongation with increasing substitution of the electrophile. It is only significant in the case of the tert-butyl fluoride, in agreement with already reported data.[21,52]

Finally, as shown in Figure 4, a very interesting trend is observed in the evolution of the SH suffered by the electrophilic center. During the previously mentioned perturbative regime, there is a significant and steady increase in the steric congestion suffered by the substrate. Such an effect arises, once again, as a direct consequence of the compression against the nucleophilic species. After this perturbative regime, the planarization of the local geometry of the substrate becomes the dominant factor, which together with the C—L bond breaking leads to a partial decongestion of the substrate. Such a result is in well agreement with previous works,[12,39,66,70] in which the effect of the planarization of carbon based species over its steric congestion was addressed. It should be noticed, however, that a slightly more complex behavior can be observed in the steric penalty of the methyl substituted species, as represented by the green curve, that exhibits a clear change in the increase rate of the steric congestion. This is in agreement with the aforementioned trends and can be attributed to the already discussed secondary effects due to the geometrical distortion of the substrate environment. Additionally, as far as the effect of the substrate is regarded, the maximum steric penalty experienced by the electrophile follows the expected trend built on the basis of chemical intuition, progressively increasing with the substitution of the electrophile on a general basis. As far as the total steric decongestion is regarded, very similar values of about −5.0 kcal/mol were found for most of the substrates, with the exception of the neopentyl moiety, that exhibits a more prominent steric relief of −18.0 kcal/mol.

## 4.2 | Effect of the nucleophile

In order to explore the effect of the steric penalty attributed to the entering nucleophile, the halogen exchange reaction of fluoromethane ($CH_3F$) with a variety of nucleophiles was employed as a model system, see Figure 6.

Generally speaking, the reaction barrier increases significantly along the halogen series, exhibiting free activation energies (see SI Section 2) of 14.5, 32.5, and 36.8 kcal/mol, respectively, and indicating that, in agreement with previously reported results,[6,24] $F^-$ is the best gas phase nucleophile among those studied. This already reported trend[6] in the activation barriers has been classically explained[4,5] attending to the evolution of the nucleophilicity along the halogen series. The aforementioned term, sometimes defined as a measure of the ability of a nucleophile to displace the leaving group, is generally considered to be dictated by the interplay between the electron density and the charge borne by the nucleophile, its electronegativity and its bulkiness. As far as SH is regarded, it is believed that as the "size" of the nucleophile increases, so will the steric penalty to be overcome in order to allow the attack to the electrophilic center. This would lead to a reduction of the effective nucleophilicity throughout the halogen series (F > Cl > Br).

The general behavior observed in the evolution of $E_{ST}^{L}$, as collected in Figure 7, is completely analogous to the one mentioned in the previous section. It exhibits the characteristic trends of both the perturbative and the planarization-distortion regimes, and hence it can be rationalized accordingly. Interestingly, a slight increase in the compression of L is observed for the heavier halogens throughout the perturbative regime, yielding maximum congestions penalties of ∼0.3, 2.0, and 2.7 kcal/mol for F, Cl, and Br, respectively. This could be rationalized in terms of the increasing size of the nucleophile, which leads to a larger compression, and hence distortion, of the electrophile skeleton in which the leaving group is embedded. Indeed, this effect is clearly reflected in the internal geometrical features of the $CH_3$ moiety, that exhibit a subtle but noticeable shortening of the H—L

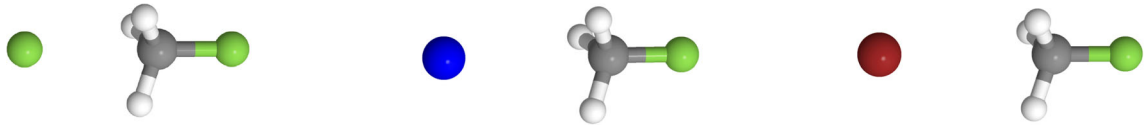

**FIGURE 6** Energetically minimized geometries, at the M06-2X/aug-cc-pVDZ level of theory in the gas phase, of the reactive complex involved in the halogen exchange reactions for different nucleophiles (F, Cl, and Br)

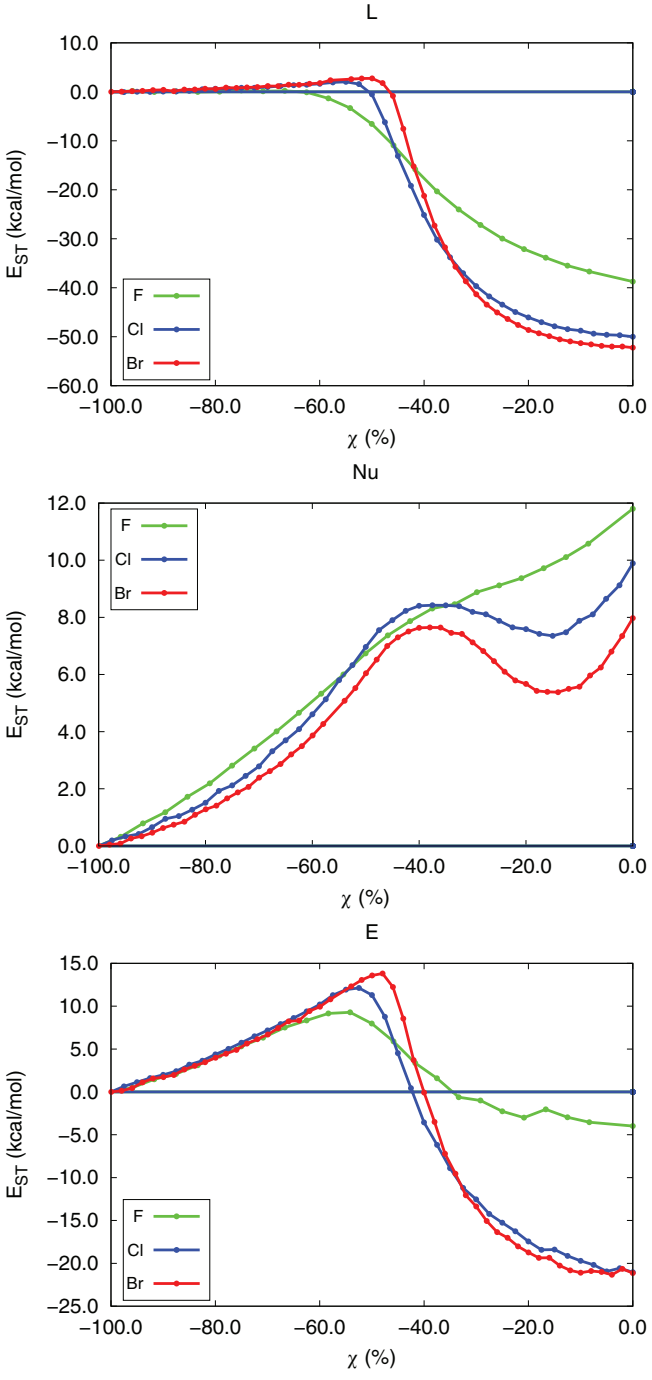


**FIGURE 7** Evolution of the steric energy $E_{ST}$ of the leaving group (top), nucleophile (center) and electrophile (bottom) throughout the $X^- + CH_3F \rightarrow CH_3X + F^-$ reaction for X = F, Cl, and Br. Calculations performed at the M06-2X/aug-cc-pVDZ level of theory in the gas phase

distance in the initial reaction stages (see SI Section 3.2). It is precisely such a decrease in the inter-atomic distance that ultimately leads to a further compression of the leaving group, something which is moreover coupled to a clear change in the rate of growth of the internal H—C—H angle, that decreases slightly along the halogen series. Furthermore, the net steric decongestion suffered by the leaving group throughout the distortion regime, as a result of the C—F bond breaking process, increases together with the bulkiness of the entering halogen. It exhibits total changes in $E_{ST}^{L}$ of −39, −50, and −52 kcal/mol for F, Cl, and Br, respectively. Such a large difference in the net steric decongestion of the leaving group can be easily rationalized as a result of the increase in the C—F distance experienced along the transition from the original ion-molecular complex to the TS structure, as reflected in Figure 8. This distance increases by roughly 0.4, 0.6, and 0.7 Å, respectively (see SI Section 3.2).

On the other hand, as far as the nucleophile is regarded, $E_{ST}^{Nu}$ increases throughout the reaction process, as expected, exhibiting once again the characteristic change in the rate of growth attributed to the electrophile planarization together with secondary decongestion phenomena. The role of this secondary effects becomes greater for the heavier halogens, for which a small valley can be observed. Such an anomalous behavior, observed for both Cl and Br is also reproduced at the HF level of theory (see SI Section 10, Figures S28–S31) and hence it should not be an artifact of the methodology. To understand it, it is wise to pay attention to the deformation of the internal H—C—H angle (see SI Section 3.2). Whereas in the case of the F nucleophile the angle increases smoothly, the reactions with Cl and Br lead to a much more abrupt and rapid increase in the internal angle of the methyl moiety, beyond the initial reaction stage. Such a rapid increase yields a much faster planarization of the system, achieving full planarity at about $\chi = -0.2$ of the reaction profile and ultimately leading to a slightly bent, not planar, TS, unlike in the case of the F atom. Such an effect can be seen in the actual geometry of the TS, as shown in Figure 8, and can be explained after taking into account the asymmetric compression experienced on the two sides of the electrophile, a result of the combination of a small leaving group (F) and progressively bulkier nucleophiles. It is precisely the relieving effect attributed to this "early planarity" that leads to a much more abrupt local steric decongestion of the nucleophile which explains the presence of the observed minimum in $E_{ST}^{Nu}$ in the Cl and Br cases. After this, the further approximation of the nucleophile towards the $CH_3$ skeleton leads to a boost in the steric compression experienced by the former. These results point out, as already suggested in the previous section, that larger nucleophiles are more likely to be affected not only by the primary compression against the central carbon atom, but

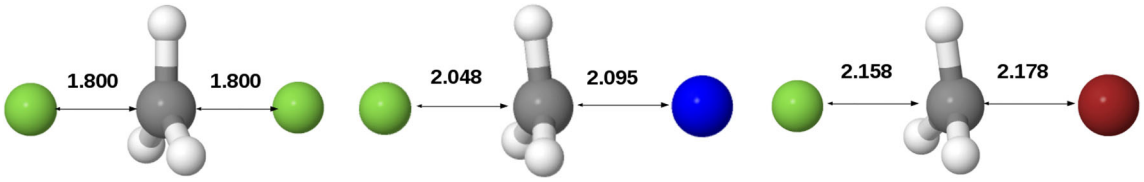


**FIGURE 8** Energetically optimized geometries, at the M06-2X/aug-cc-pVDZ level of theory in the gas phase, of the transition state involved in the halogen exchange reactions for different nucleophiles (F, Cl, and Br). Bond distances are given in Å. Further details can be found in SI (Tables S3–S10)

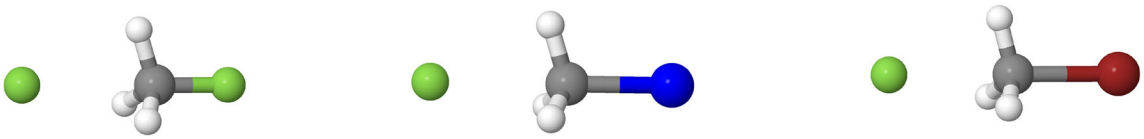

**FIGURE 9** Energetically minimized geometries, at the M06-2X/aug-cc-pVDZ level of theory in the gas phase, of the reactive complexes involved in the halogen exchange reactions for different leaving groups (F, Cl, and Br)

also by secondary compression phenomena with its vicinal groups, something which becomes exacerbated along the halogen series. Furthermore, the total steric penalty suffered by the nucleophile decreases throughout the F, Cl, and Br series, in agreement with the aforementioned discussions but against classical chemical intuition. Finally, and as it can be seen in Figure 7, the steric energy experienced by the $CH_3$ skeleton along the reaction follows the expected trend, exhibiting an almost linear increase in the perturbative regime (mainly due to the E-Nu compression) that is followed by a subsequent decongestion of the electrophile. Moreover, the maximum steric penalty suffered by the organic scaffold increases throughout the halogen series, peaking at 9.3, 12.1, and 13.8 kcal/mol for F, Cl, and Br, respectively. Such a trend provides a chemically appealing picture and can be understood considering the further compression undergone by both the central C atom and its vicinal groups with the increasing size of the nucleophile, inherent to the halogen series. After passing the perturbative regime the total release of steric congestion of the substrate, arising from its geometrical distortion, reaches values of −4.0, −21.0, and −21.1 kcal/mol for the F, Cl, and Br nucleophiles. According to our interpretation, the original $CH_3F$ skeleton undergoes a very strong distortion accompanying the C-F bond breaking process. It is the increase in the rate of bond lengthening (see SI Section 3.2) when the attacking halogen changes that results in a much more prominent steric decongestion and a larger stabilizing $E_{ST}$ value for the electrophile. Moreover, the discrepancies observed between fluorine and the remaining halogens are in agreement with the very well-known unique behavior of the F atom, which has been claimed to arise from the charge-shift nature of fluorine containing bonds.[11,71,72]

## 4.3 | Effect of the leaving group

Finally, with the aim to assess the steric effects attributed to the nature of the leaving group, the halogen exchange reaction of fluoro-, chloro- and bromo-methane ($CH_3F$, $CH_3Cl$, and $CH_3Br$) with the fluoride anion ($F^-$) was evaluated, see Figure 9. Notice that the transition states are the same as the previously discussed ones, as represented in Figure 8.

Contrary to the previous section, the free activation energies decrease significantly along the halogen series, showing $\Delta G^{\ddagger}$ values of 14.5, 3.4, and 0.8 kcal/mol, respectively (see SI Section 2) and leading to an almost barrierless process in the case of the heaviest halogen (Br). These monotonously decreasing trend is in accordance with chemical intuition and already reported data[6] and it is claimed to arise from the increase in the leaving group ability across the F, Cl, and Br series. It has been suggested[4,73] that the major factor controlling the leaving group ability in the gas phase is actually the interplay between the basicity of L together with the strength of the C—X bond. It is precisely the bond lengthening and weakening experienced by the C—X bond through the halogen series that has been employed to explain the observed trends.

Once again, and as collected in Figure 10, the evolution of the steric energy experienced by the leaving group is in accordance with the already mentioned trends, although there are some remarkable differences with the change of the nature of the leaving group. The duration of the perturbative regime is clearly diminished with respect to that of the previous sections, almost vanishing in the case of Br. This correlates with the increase in the leaving group ability and it is also directly reflected in the evolution of the C-L bond length (see SI Section 3.3), which undergoes a noticeable lengthening even in the early stages of the reaction for Cl and Br. On the other hand, the total steric decompression experienced by L becomes severely reduced, following a similar trend to that observed in the maximum distortion of the C—L bond distances, with values of 0.36, 0.22, and 0.12 Å along the halogen series. This progressively smaller bond elongation, inherent to the transition from reactants to the TS, gives rise to a softer decompression phenomena, thus, explaining the observed trends in $E_{ST}$. The previous observation is coupled to a remarkably slow distortion of the methyl moiety, as reflected by the evolution of

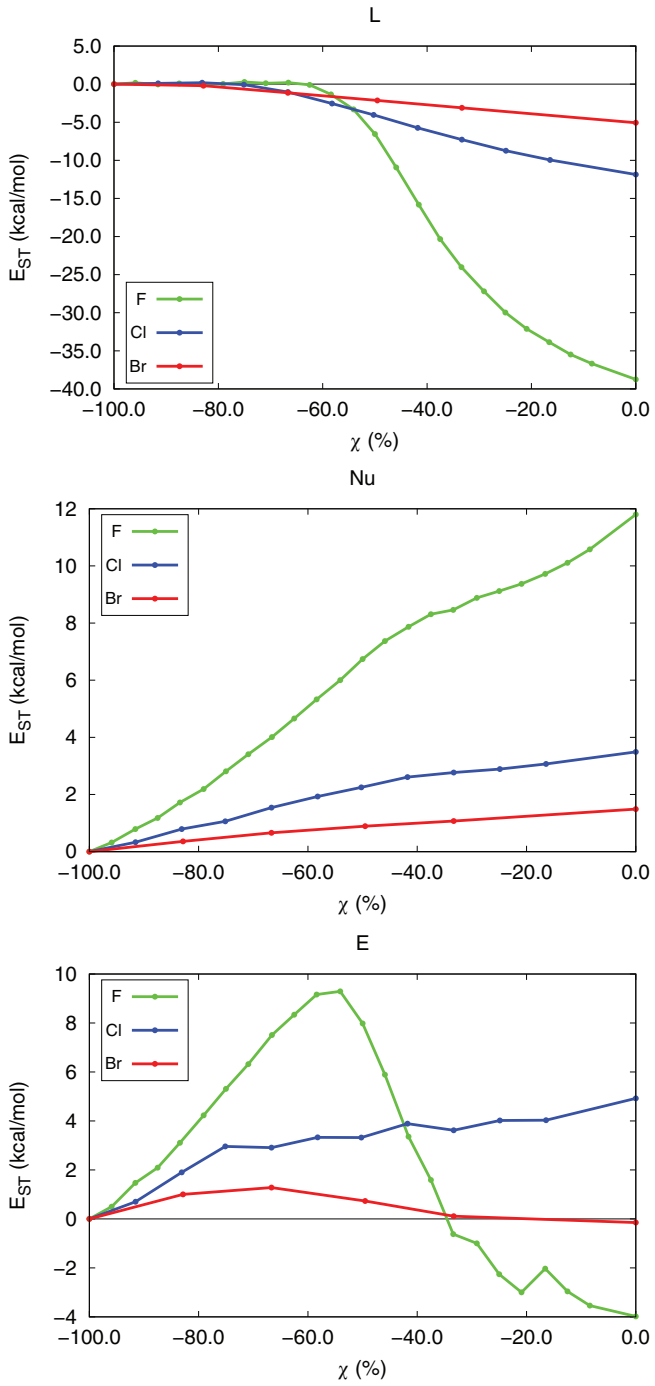


**FIGURE 10** Evolution of the steric energy $E_{ST}$ of the leaving group (top), nucleophile (center) and electrophile (bottom) throughout the $F^- + CH_3X \rightarrow CH_3F + X^-$ reaction for X = F, Cl, and Br. Calculations performed at the M06-2X/aug-cc-pVDZ level of theory in the gas phase

the H—C—H angle (SI Section 3.3). This leads to far from planar activation complex structures, in agreement with the Hammond postulates and already reported data[24]: the reactions are exothermic, and hence the TS structure is prone to resemble the structure of the starting reactive complex.

Similarly, the steric energy experienced by the nucleophile (F) evolves as expected, increasing through the progress of the reaction. However, the total compression suffered by it decreases significantly through the halogen series, exhibiting maxima of 11.8, 3.5, and 1.5 kcal/mol, respectively. This intriguing result can be rationalized as the outcome of the much more moderate nucleophile to electrophile compression suffered through the halogen series, that yields a C—Nu distance in the activation complex structure of 1.8, 2.0 and 2.15 Å for the F, Cl, and Br atoms, respectively. Moreover, the evolution of the H—C—H angle (see SI Section 3) reveals that, though the full planarity of the methyl moiety is not achieved for L = Cl or Br, the larger size of the leaving group imposes a considerably wider internal angle in the starting complex and consequently the nucleophile is compressed up to a lower extent by the vicinal groups to the electrophilic center. Additionally, and unlike in the previous scenarios, the rate of increase of the steric congestion of the nucleophile becomes almost uniform in the F, Cl, and Br series, in accordance with the much smoother planarization rate of the methyl moieties. This makes the Nu—C confinement the most dominant factor determining the Nu compression throughout the entire substitution reaction for the heavier analogs.

As far as the substrate is regarded, a very interesting trend is observed. The maximum congestion penalty of the substrate decreases through the halogen series, exhibiting values of 9.3, 4.9, and 1.3 kcal/mol, respectively. This can be rationalized attending to the already mentioned increasing C—Nu and C—L distances at the, almost symmetric, activation complex structure. That yields progressively larger C—X distances as the size of the halogen (X) increases. This suggests that the confinement undergone by the electrophile along the reaction becomes, on average, less prominent as the size of the leaving group is increased. These results are biased by the difference in the early stages of the reaction; Whereas a well-defined perturbative regime (within which the C—L bond distance is barely modified) exists in the case of F, the much earlier, and yet smoother, extrusion of the leaving group for Cl and Br leads to slightly reduced electrophile compression. Our results show that the total steric decongestion of the electrophile becomes less clear along the halogen series, a result of the much subtle and earlier internal geometrical distortion of the substrates along the group. Moreover, the F atom seems again to behave differently to its heavier analogs.

## 5 | CONCLUSIONS

Chemical intuition often considers SH as one of the crucial driving forces determining the outcome of multiple chemical phenomena, including the archetypal case of $S_N2$ reactions. Unfortunately, the lack of rigor inherent to chemical thinking, limits the validity of these arguments. In this work, we have thoroughly explored the SH undergone throughout different gas-phase $S_N2$ reactions taking place between simple electrophiles and halides. Some relevant conclusions can be distilled from our results:

- As far as the substrate is regarded, and with the particular exception of the neopentyl group, the steric compression undergone by

the electrophile during the initial stages of the reaction shows an increasing trend with the bulkiness of the substrate, in agreement with the trends followed by the activation barriers.

- Generally speaking, steric clashes become more sensitive to the surrounding chemical environment as the bulkiness of the chemical species under consideration increases. Thus, for instance, along the F > Cl > Br series the contribution of secondary effects to the SH of the halogens becomes larger.
- On the transition from reactants to the activated complex, the evolution of $E_{ST}^{Nu}$ is more susceptible to a change in the decoration of the organic skeleton than $E_{ST}^{L}$, this being a direct consequence of the backside attack accompanying the studied $S_N2$ mechanism. Similarly, for small enough Nu or L, the SH seems to arise almost entirely from the direct clashing against the central C atom, being thus quite unaffected by the substitution of the electrophile.
- Counterintuitively, the electrophilic skeleton generally experiences a subtle compression followed by a moderate steric relief. This results from the interplay between a penalizing nucleophile compression and a relieving electrophile planarization.
- Although, as expected, "larger" species would generally result in significant steric compression along a chemical transformation, changes in interatomic distances can yield relevant deviations of $E_{ST}$ from the classically expected trends. As an example, increasing the size of the extruding leaving group (L) results in smaller decompressions of the latter. This is a manifestation of the non-negligible effect of the variable elongation of the C—L bond with the nature of L.
- In agreement with the well-known peculiar nature of the F atom within the halogens group, its $E_{ST}^{F}$ shows a somehow distinctive behavior when compared to that of Cl or Br.
- As far as the neopentyl group ($(CH_3)_3CCH_2$—) is regarded, the behavior of its $E_{ST}$ fits the general trends found for the remaining substrates. However $E_{ST}^{E}$ experiences a specially pronounced steric decompression during the evolution from the starting reactive complex to the TS. This is attributed to the larger "in-molecule" steric strain inherent to the neopentyl fluoride skeleton, which is attenuated by the planarization phenomenon.

Our results point out that the IQA description of SH matches almost perfectly the trends expected from chemical intuition in $S_N2$ reactions, reinforcing its validity as a measure of SH. We emphasize that SH should never be the only argument used to rationalize the easiness of $S_N2$ reactions. Additionally, the steric clashing between two moieties A and B is not necessarily symmetric and special care must be taken when using chemically intuitive SH arguments to understand chemical phenomena. Altogether, the results of this work show that, formally speaking, the concept of SH as it is usually formulated in chemistry can only be isolated from other effects for perturbative like regimes where, indeed, our $E_{ST}$ descriptor seems to follow the trends in reactivity dictated by chemical intuition. On the other hand, the classical picture of SH blurs in strong distortion regimes, such as those found in the vicinity of transition states, where major electronic structure changes make it difficult to tell it from other contributions. Instead, it is likely that in these strongly interacting situations the effects of charge transfer phenomena have been incorrectly attributed to SH. We would also like to highlight that, within the IQA approach, $E_{ST}$ is only one of the three contributions, along with the $E_{int}$ and $E_{CT}$ terms that build up the total energy, suggesting that predicting changes in the latter under the narrow perspective of only one of its components (as it is often the case when SH arguments are used) offers a strongly biased, to say the least, picture of chemistry.

## ACKNOWLEDGMENTS

We thank the Spanish MICINN, grant PGC2018-095953-B-I00, for financial support, M.G specially thanks the Spanish MICIU and MIU for the predoctoral FPU grant, FPU19/02903.

## DATA AVAILABILITY STATEMENT

Data available on request from the authors. The data that support the findings of this study are available from the corresponding author upon reasonable request.

## ORCID

*Miguel Gallegos* https://orcid.org/0000-0001-7472-8158
*Aurora Costales* https://orcid.org/0000-0003-3815-8447
*Ángel Martín Pendás* https://orcid.org/0000-0002-4471-4000

## ENDNOTE

[1] The "bulkier" and "closer" an species is, the larger it will be its ability to induce steric hindrance.

## REFERENC

[1] Y. Han, J.-R. Li, Y. Xie, G. Guo, *Chem. Soc. Rev.* **2014**, *43*, 5952.
[2] J. F. Bunnett, R. E. Zahler, *Chem. Rev.* **1951**, *49*, 273.
[3] G. C. Fu, *ACS Cent. Sci.* **2017**, *3*, 692.
[4] K. Vollhardt, N. Schore, *Organic Chemistry, Fourth Edition: Structure and Function*, W. H. Freeman, New York **2003**.
[5] C. K. Ingold, in *Structure and mechanism in organic chemistry* (Ed: G. Bell) Cornell University Press, Ithaca **1953**.
[6] T. A. Hamlin, M. Swart, F. M. Bickelhaupt, *ChemPhysChem* **2018**, *19*, 1315.
[7] I. Szabó, G. Czakó, *Nat. Commun.* **2015**, *6*, 6.
[8] C. H. DePuy, S. Gronert, A. Mullin, V. M. Bierbaum, *J. Am. Chem. Soc.* **1990**, *112*, 8650.
[9] J. K. Laerdahl, E. Uggerud, *Int. J. Mass Spectrom.* **2002**, *214*, 277.
[10] M. N. Glukhovtsev, B. A. Pross, L. Radom, *J. Am. Chem. Soc.* **1995**, *117*, 2024.
[11] I. Alkorta, J. C. R. Thacker, P. L. A. Popelier, *J. Comput. Chem.* **2018**, *39*, 546.
[12] M. Gallegos, A. Costales, A. Martín Pendás, *ChemPhysChem* **2021**, *22*, 775.
[13] R. R. Holmes, *Chem. Rev.* **1990**, *90*, 17.
[14] S. M. Bachrach, J. T. Woody, D. C. Mulhearn, *J. Org. Chem.* **2002**, *67*, 8983.
[15] O. I. Kolodiazhnyi, A. Kolodiazhna, *Tetrahedron: Asymmetry* **2017**, *28*, 1651.
[16] M. Bortoli, L. P. Wolters, L. Orian, F. M. Bickelhaupt, *J. Chem. Theory Comput.* **2016**, *12*, 2752.

[17] S. Wolfe, D. J. Mitchell, H. B. Schlegel, *J. Am. Chem. Soc.* **1981**, *103*, 7692.
[18] X. Ma, G. Di Liberto, R. Conte, W. L. Hase, M. Ceotto, *J. Chem. Phys.* **2018**, *149*, 164113.
[19] K. Morokuma, *J. Am. Chem. Soc.* **1982**, *104*, 3732.
[20] J. J. Wolff, *Am. Ethnol.* **1993**, *105*, 1277.
[21] F. Jensen, *Chem. Phys. Lett.* **1992**, *196*, 368.
[22] M. N. Glukhovtsev, A. Pross, L. Radom, *J. Am. Chem. Soc.* **1996**, *118*, 6273.
[23] S. Giri, E. Echegaray, P. W. Ayers, A. S. Nuñez, F. Lund, A. Toro-Labbé, *J. Phys. Chem. A* **2012**, *116*, 10015.
[24] M. Capurso, R. Gette, G. Radivoy, V. Dorn, *Proceedings* **2019**, *41*, 41.
[25] L. Sun, K. Song, W. L. Hase, *Science* **2002**, *296*, 875.
[26] J. Xie, W. L. Hase, *Science* **2016**, *352*, 32.
[27] I. Szabó, H. Telekes, G. Czakó, *J. Chem. Phys.* **2015**, *142*, 244301.
[28] D. Papp, G. Czakó, *Chem. Sci.* **2021**, *12*, 5410.
[29] Y. Wang, H. Song, I. Szabó, G. Czakó, H. Guo, M. Yang, *J. Phys. Chem. Lett.* **2016**, *7*, 3322.
[30] I. Szabó, G. Czakó, *J. Phys. Chem. A* **2017**, *121*, 9005.
[31] E. Carrascosa, J. Meyer, J. Zhang, M. Stei, T. Michaelsen, W. L. Hase, L. Yang, R. Wester, *Nat. Commun.* **2017**, *8*, 8.
[32] E. Carrascosa, J. Meyer, T. Michaelsen, M. Stei, R. Wester, *Chem. Sci.* **2018**, *9*, 693.
[33] J. Zhang, U. Lourderaj, R. Sun, J. Mikosch, R. Wester, W. L. Hase, *J. Chem. Phys.* **2013**, *138*, 114309.
[34] R. Wester, A. E. Bragg, A. V. Davis, D. M. Neumark, *J. Chem. Phys.* **2003**, *119*, 10032.
[35] L. B. Young, E. Lee-Ruff, D. K. Bohme, *J. Chem. Soc. Chem. Commun.*, **1973**, *973*, 35b.
[36] J. L. Beauchamp, M. C. Caserio, T. B. McMahon, *J. Am. Chem. Soc.* **1974**, *96*, 6243.
[37] D. K. Bohme, G. I. Mackay, J. D. Payzant, *J. Am. Chem. Soc.* **1974**, *96*, 4027.
[38] S. E. Barlow, J. M. V. Doren, V. M. Bierbaum, *J. Am. Chem. Soc.* **1988**, *110*, 7240.
[39] I. Fernández, G. Frenking, E. Uggerud, *Chem. Eur. J.* **2009**, *15*, 2166.
[40] W. J. van Zeist, F. Bickelhaupt, *Chem. Eur. J.* **2010**, *16*, 5538.
[41] I. Dostrovsky, E. D. Hughes, C. K. Ingold, *J. Chem. Soc.* **1946**, *0*, 173.
[42] G. Frenking, A. Krapp, *J. Comput. Chem.* **2007**, *28*, 15.
[43] B. C. B. Symons, D. J. Williamson, C. M. Brooks, A. L. Wilson, P. L. A. Popelier, *ChemistryOpen* **2019**, *8*, 560.
[44] J. K. Badenhoop, F. Weinhold, *J. Chem. Phys.* **1997**, *107*, 5406.
[45] J. K. Badenhoop, F. Weinhold, *J. Chem. Phys.* **1997**, *107*, 5422.
[46] J. Dillen, *Int. J. Quantum Chem.* **2013**, *113*, 2143.
[47] C. Colwell, T. Price, T. Stauch, R. Jasti, *Chem. Sci.* **2020**, *11*, 3923.
[48] M. Blanco, A. Martín Pendás, E. Francisco, *J. Chem. Theory Comput.* **2005**, *1*, 1096.
[49] D. M. Andrada, C. Foroutan-Nejad, *Phys. Chem. Chem. Phys.* **2020**, *22*, 22459.
[50] J. Chandrasekhar, S. F. Smith, W. L. Jorgensen, *J. Am. Chem. Soc.* **1984**, *106*, 3049.
[51] J. M. Garver, Y. Ren Fang, N. Eyet, S. M. Villano, V. M. Bierbaum, K. C. Westaway, *J. Am. Chem. Soc.* **2010**, *132*, 3808.
[52] A. A. Mohamed, F. Jensen, *J. Phys. Chem. A* **2001**, *105*, 3259.
[53] Francisco, E.; Martín Pendás, A. In *Non-Covalent Interactions in Quantum Chemistry and Physics*; Otero de la Roza, A., DiLabio, G. A., Eds.; Elsevier, Amsterdam **2017**; pp. 27–64.
[54] F. Weinhold, C. R. Landis, *Chem. Educ. Res. Pract.* **2001**, *2*, 91.
[55] M. V. Hopffgarten, G. Frenking, *WIREs Comput. Mol. Sci* **2012**, *2*, 43.
[56] R. Bader, *Atoms in Molecules: A Quantum Theory*; *International Series of Monographs on Chemistry*, Clarendon Press, Oxford **1990**.
[57] R. Parr, W. Yang, *Density Fucntional Theory of Atoms and Molecules*; *International Series of Monographs on Chemistry*, Oxford University Press, New York, Oxford **1989**.
[58] M. J. Frisch, G. W. Trucks, H. B. Schlegel, G. E. Scuseria, M. A. Robb, J. R. Cheeseman, G. Scalmani, V. Barone, G. A. Petersson, H. Nakatsuji, X. Li, M. Caricato, A. Marenich, J. Bloino, B. G. Janesko, R. Gomperts, B. Mennucci, H. P. Hratchian, J. V. Ortiz, A. F. Izmaylov, J. L. Sonnenberg, D. Williams-Young, F. Ding, F. Lipparini, F. Egidi, J. Goings, B. Peng, A. Petrone, T. Henderson, D. Ranasinghe, V. G. Zakrzewski, J. Gao, N. Rega, G. Zheng, W. Liang, M. Hada, M. Ehara, K. Toyota, R. Fukuda, J. Hasegawa, M. Ishida, T. Nakajima, Y. Honda, O. Kitao, H. Nakai, T. Vreven, K. Throssell, J. A. Montgomery, Jr., J. E. Peralta, F. Ogliaro, M. Bearpark, J. J. Heyd, E. Brothers, K. N. Kudin, V. N. Staroverov, T. Keith, R. Kobayashi, J. Normand, K. Raghavachari, A. Rendell, J. C. Burant, S. S. Iyengar, J. Tomasi, M. Cossi, J. M. Millam, M. Klene, C. Adamo, R. Cammi, J. W. Ochterski, R. L. Martin, K. Morokuma, O. Farkas, J. B. Foresman, and D. J. Fox. Gaussian 09 Revision E.01, Gaussian Inc, Wallingford CT **2009**.
[59] Martín Pendás, A.; Francisco, E. Promolden. A QTAIM/IQA code (Avaliable from the authors upon request).
[60] Y. Zhao, D. G. Truhlar, *Theor. Chem. Acc.* **2008**, *120*, 215.
[61] W. N. Olmstead, J. I. Brauman, *J. Am. Chem. Soc.* **1977**, *99*, 4219.
[62] G. Caldwell, T. F. Magnera, P. Kebarle, *J. Am. Chem. Soc.* **1984**, *106*, 959.
[63] G. Vayner, K. N. Houk, W. L. Jorgensen, J. I. Brauman, *J. Am. Chem. Soc.* **2004**, *126*, 9054.
[64] M. S. Newman, *Steric Effects in Organic Chemistry*, Wiley, London: Chapman & Hall **1956**.
[65] D. F. DeTar, N. P. Luthra, *J. Am. Chem. Soc.* **1980**, *102*, 4505.
[66] I. Fernández, G. Frenking, E. Uggerud, *Chem. Eur. J.* **2010**, *16*, 5542.
[67] E. Uggerud, *Pure Appl. Chem.* **2009**, *81*, 709.
[68] S. Liu, H. Hu, L. G. Pedersen, *J. Phys. Chem. A* **2010**, *114*, 5913.
[69] E. D. Hughes, C. K. Ingold, J. D. H. Mackie, *J. Chem. Soc. (Resumed)* **1955**, *3177*, 3177.
[70] F. M. Bickelhaupt, T. Ziegler, P. Schleyer, v. R., *Organometallics* **1996**, *15*, 1477.
[71] S. Shaik, D. Danovich, B. Silvi, D. L. Lauvergnat, P. C. Hiberty, *Chem. – Eur. J.* **2005**, *11*, 6358.
[72] E. Espinosa, I. Alkorta, J. Elguero, E. Molins, *J. Chem. Phys.* **2002**, *117*, 5529.
[73] M. Stei, E. Carrascosa, M. A. Kainz, A. H. Kelkar, J. Meyer, I. Szabó, G. Czakó, R. Wester, *Nat. Chem.* **2016**, *8*, 151.

## SUPPORTING INFORMATION

Additional supporting information may be found in the online version of the article at the publisher's website.

**How to cite this article:** M. Gallegos, A. Costales, Á. Martín Pendás, *J. Comput. Chem.* **2022**, *43*(11), 785. https://doi.org/10.1002/jcc.26834